

A Hybrid Geometric Optical-Radiative Transfer Approach for Modeling Albedo and Directional Reflectance of Discontinuous Canopies

Xiaowen Li, Alan H. Strahler, *Member, IEEE*, and Curtis E. Woodcock

Abstract—A new model for the bidirectional reflectance of a vegetation cover combines principles of geometric optics and radiative transfer. It relies on gap probabilities and path length distributions to model the penetration of irradiance from a parallel source and the single and multiple scattering of that irradiance in the direction of an observer. The model applies to vegetation covers of discrete plant crowns that are randomly centered both on the plane and within a layer of variable thickness above it. Crowns assume a spheroidal shape with arbitrary height to width ratio. Geometric optics easily models the irradiance that penetrates the vegetation cover directly, is scattered by the soil, and exits without further scattering by the vegetation. Within a plant crown, the probability of scattering is a negative exponential function of path length. Within-crown scattering provides the source for singly-scattered radiation, which exits with probabilities proportional to further path-length distributions in the direction of exitance (including the hotspot effect). Single scattering provides the source for double scattering, and then higher order pairs of scattering are solved successively by a convolution function. Early validations using data from a conifer stand near Howland, Maine, show reasonable agreement between modeled and observed reflectance.

I. INTRODUCTION

THE purpose of this paper is to present a new model for the directional reflectance of vegetation canopies and to show some initial results from attempts to validate the model using data currently available. The new model draws heavily from past work in geometric optics, and also includes multiple scattering effects in a manner similar to radiative transfer models—hence the new model's description as a hybrid geometric-optical radiative-transfer model. Additionally, the model is formulated explicitly to deal with discontinuous canopies, where the presence of gaps in the canopy has significant effects on both the amount of irradiance passing directly through the canopy and the directional reflectance of the canopy—and in particular, the hotspot. Thus, gap probabilities play a major role in this new model by influencing the calculation of the distribution of pathlengths through the canopy, the distribution of single-scattering source radiation, and the calculation of an openness factor which is used to

model multiple scattering and the scattering of the diffuse sky irradiance.

The scene model underlying this new hybrid model is the same discrete-object model used in our previous work on geometric optics [1], [2]. The scene is composed of three-dimensional objects, which in this case are individual plant crowns, that when taken together comprise the plant canopy. Their shapes, size, and count density are all important parameters describing the scene. This scene model contrasts significantly with plane-parallel models for canopies, and is particularly suited for discontinuous plant canopies. The new hybrid model is designed for use at the scale of patches of vegetation, or areas large enough to be characterized by the means of parameters, but also homogeneous enough that those means exhibit stationarity. For forests, which have served as the primary environment driving the development of this model, the appropriate scale of application is a forest stand, which could range in area from a single hectare to tens or hundreds of hectares.

The primary focus of this paper concerns the use of the new hybrid model for studying the directional reflectance and albedo of plant canopies. However, the model also allows for calculation of a wide variety of radiation quantities as a function of height in the canopy. Thus, the model should also prove useful for studies of surface energy balance and a variety of canopy processes, such as photosynthesis and transpiration.

II. BACKGROUND

The modeling of directional reflectance of vegetated surfaces is at present a highly active research field. The research in this area is extensive and has been recently reviewed. [3]–[6]. For the purposes of this paper, two approaches to modeling reflectance are of particular relevance: radiative transfer and geometric optics. In the radiative transfer approach, the vegetation canopy is treated as a volume-scattering medium using principles and physical approximations originally developed for the atmosphere. Typically, leaves are taken as discrete scattering elements. The approach requires determination of a number of physical constants that describe leaf characteristics, such as their scattering phase function and single scattering albedo, and other constants that describe their structure, such as leaf size and shape, leaf area index, and leaf angle distribution [7]. Usually a plane-parallel leaf canopy is assumed, which is more appropriate for crop canopies than

Manuscript received September 14, 1993; revised September 6, 1994. This work was supported in part by the National Aeronautics and Space Administration under contract NAS5-31369; in part by the National Science Foundation of the United States under Grant INT-9014263; and in part by the National Science Foundation of China under Grants 4880050 and 49331020.

The authors are with the Center for Remote Sensing, Boston University, Boston, MA 02215 USA.

IEEE Log Number 9407848.

natural vegetation canopies, which exhibit gaps and openings. Some models based on radiative transfer have included three-dimensional effects, as well as geometric-optical principles, to describe single-scattering behavior [8].

The radiative transfer approach is probably the most accurate at modeling reflectance at the micro scale, but also requires the most calibration. Further, the computational load is often large when the radiative transfer equation is to be solved with high accuracy. Another difficulty lies in validation, which requires careful measurements of radiances as well as simultaneous measurements of numerous leaf and canopy parameters and downwelling directional irradiance. Ground-based measurements of crop canopies are typically used, as collected, for example, by the PARABOLA instrument [9]. These factors contribute to making the use of models based on the radiative transfer equation impractical for applications at landscape scales.

In the geometric-optical approach, the reflectance is modeled as a function of the self-shadowing structure of the canopy, which is treated as a collection of discrete objects—individual plant crowns—that are arranged on a plane. The pattern of sunlit and shadowed objects and background that is seen from a particular viewing position is taken as the primary factor controlling the directional reflectance [1], [2]. The pattern of light and shade associated with the scene is modeled using geometric optics, Boolean set mathematics, and theorems from stereology [10]–[12]. Originally developed as a practical alternative to radiative transfer models for complex, naturally-vegetated land surfaces that cannot be approximated as plane-parallel canopies, the geometric-optical approach has been extended to leaves as objects in both plane-parallel and discrete canopies [13], [14]. In essence, the geometric-optical approach amounts to a careful description of single scattering with a very simplified treatment of multiple scattering. A similar approach to modeling for directional reflectance of forest covers was developed independently by Estonian researchers in the former USSR [15], [16] and became available in the western literature at about the same time as our publications [17]. Though these two approaches share some similarity, they have also significant differences. Notably, we tend to clearly distinguish intercrown and between-crown gaps and to emphasize the importance of K_c , the proportion of the sunlit and viewed crown surface. This enables us to treat mutual shadowing and the directional effect of clumping properly.

Validation of geometric-optical models is generally easier than validation of other types, since the canopy parameters and component radiances are not difficult to measure. Aircraft instruments, such as the Advanced Silicon Array Spectrometer [18], which can make directional measurements of radiances over large vegetated areas, can provide suitable data if corrected for atmosphere effects [19].

The intent of the new hybrid model is to incorporate the strengths of both approaches, which is a careful description of single scattering from geometric-optics, and the effects of higher orders of scattering from radiative transfer theory. The result of this combination should be an accurate model of the full range of quantities addressable via radiative transfer, while

continuing to be applicable for discontinuous canopies and at landscape scales.

III. GAP PROBABILITIES IN VEGETATION CANOPIES

Gap probability is the probability that a photon incident upon a vegetation canopy will pass directly through the canopy without being intercepted by a leaf, branch, or stem. Typical models for gap probability are of the form

$$P_{\text{gap}} = e^{-kL_f \cos \theta} \quad (1)$$

where L is the leaf area index, k is the fraction of the foliage area projected toward the angle of incidence, and θ is the zenith angle of incidence. This model has been widely used for homogeneous vegetation canopies [20].

Most real vegetation canopies, and especially canopies of arboreal vegetation covers, depart significantly from this simple model. A significant part of the total gap will be present as gaps between individual crowns, which we have previously termed as $P(n = 0)$, where n is the number of plant crowns penetrated by a ray, and modeled as a function of crown size, shape, and count density. Besides these intercrown gaps, we explicitly modeled within-crown $P_{\text{gap}}(s)$ as a function of the within-crown pathlength s at the scale of leaves [21]

$$p_{\text{gap}}(s, \theta) = e^{-s k(\theta) D_v}. \quad (2)$$

Here, $k(\theta)$ is the leaf area projection factor for the direction θ ; D_v is the foliage area volume density (FAVD) with units m^{-1} . Unless otherwise mentioned, we'll assume the leaf area is uniformly distributed within the crowns, and thus D_v is constant within crowns, zero outside. We'll use $\tau(\theta) = k(\theta) D_v$ as a parameter describing projected foliage density in the direction θ . This equation is very similar to (1) in form, but it explicitly discards the assumption of a horizontal layer implied in (1). Hence it is available for dealing with various canopy structures through the distribution of pathlengths s given the geometry/structure of an average single crown. Then the mean P_{gap} over an area A becomes

$$\begin{aligned} E(P_{\text{gap}}) &= \frac{1}{A} \iint_A e^{-\tau(\theta)s(x,y)} dx dy \\ &= \int_0^\infty P_{\text{gap}}(s(\theta)) P(s(\theta)) ds(\theta). \end{aligned} \quad (3)$$

Here, $P(s)$ denotes probability density function of s ; similarly we will use $P(y | x)$ for probability density function of y given condition x in the latter text.

Note that since P_{gap} determines the proportion of radiation flux that is not scattered by foliage, $(1 - P_{\text{gap}})$ will be the fraction of the incoming flux reflected, transmitted, or absorbed by foliage. After interception, the reflected and transmitted light become scattered flux into other directions and further scattering/absorption is again determined by the exit-pathlength distribution and its correlation to the incoming-pathlength distribution. Hence, the modeling of P_{gap} becomes a key linking geometric-optical and radiative-transfer models of 3-D discrete crown canopies.

A typical 1-D radiative transfer equation for a horizontally homogeneous and infinite canopy is often applied to solve for

$I(z, \Omega)$, the specific energy intensity at given direction and solid angle Ω , at given wavelength in absence of polarization. Usually we can decompose I into uncollided I_0 and scattered components I_1, I_2, \dots in successive order, and apply the equation only to two successive orders of scattering iteratively, starting from attenuation only for I_0 , which is

$$\begin{aligned} I_0(x, y, z) &= I_{\text{sun}}(\theta_i) e^{-\tau s(x, y, z, \theta_i)} \\ &= I_{\text{sun}}(\theta_i) P_{\text{gap}}(s(x, y, z, \theta_i)) \end{aligned} \quad (4)$$

where $I_{\text{sun}}(\theta_i)$ is specific energy intensity and is assumed to be the only external radiance from zenith angle θ_i above the canopy, the canopy is assumed azimuthally isotropic and the solar azimuthal angle ϕ_i is omitted for simplicity; τ is assumed constant, and s is the within-canopy pathlength for the raybeam at the given direction to reach the point (x, y, z) . Equation (4), like (1), can be obtained from either the radiative transfer equation under given conditions or from pure statistical geometry.

In this model, we are not interested in uncollided radiance at each point, but rather in its probability distribution at the height h —that is, $P(I_0 | h, \theta_i)$. Given the height, (4) tells us that I_0 at every point (x, y, z) is a monotone function of the pathlength at that point, hence the distribution of I_0 at the height h can be obtained from the probability density distribution of the pathlengths s at h , or $P(s | h, \theta_i)$. Our model does not treat I_0 as x, y independent as in a 1-D homogeneous layer model, nor do we need to calculate exactly its value at every x, y, z as in some 3-D models. Instead we only need to calculate $P(s | h, \theta_i)$.

Further, after we have distribution of I_0 with height, we can obtain the distribution of the fraction of beam irradiance with height that collides with leaf canopy material. The unabsorbed proportion of that irradiance is scattered, thus providing the distribution of single-scattering source radiance.

IV. THE VERTICAL DISTRIBUTION OF SUNLIT CROWN SURFACE

In order to calculate $P(s | h, \theta_i)$, we need first to obtain the probability that a solar raybeam will reach a point at height h without hitting any crown $P(n = 0 | h, \theta_i)$. This is pure geometric statistics. By definition, at any point directly reached by a solar raybeam, the within-crown pathlength at this point is zero, and there is no scattering before the raybeam reaches this point. But at this point, the solar raybeam may or may not enter a crown. In the former case, the pathlength is also zero but the raybeam starts the scattering process. In order to make expressions simpler, from now on, we will exclude the case $n = 0$ from all probability distributions of s or I_0 or example, $P(s = 0 | h, \theta_i)$, does not include $P(n = 0 | h, \theta_i)$, but the probability that a raybeam first enters a crown. The only exception to this is for points on the ground, where a solid surface is assumed.

In this section, we'll assume that the foliage is contained in spherical crowns of radius R . Since the spherical model can be easily extended to the spheroid model [21], this assumption will not cause the model to lose generality. Given the 3-D distribution of crown centers and the geometry of crowns

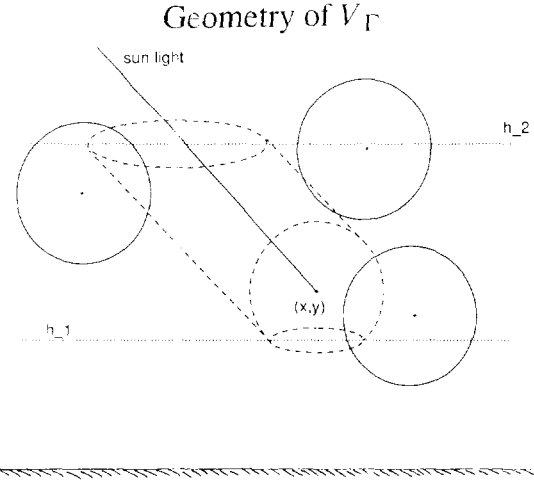


Fig. 1. Geometry of V_F . If and only if there are no crown centers (cross) in V_F (volume enclosed by dashed lines), the point (x, y) can be reached by direct sunlight without penetrating other crowns (solid circles).

at the ground surface ($h = 0$), $P(n = 0 | h = 0, \theta_i)$ has been well modeled [13], [21]. This corresponds to solving for the proportion of sunlit background. If the crown centers are distributed at the same height H , $P(n = 0 | h, \theta_i)$ has also been obtained for all heights h [2]. In the case that the crown centers are distributed between a lower boundary h_1 and an upper boundary h_2 , $P(n = 0 | h, \theta_i)$ for any h ranging from $h_1 - R$ to $h_2 + R$ can be obtained as follows.

Assuming that a point at height h receives a direct irradiance from direction θ_i , then there must be no crown centers within the volume of a crown sphere centered at this point, otherwise the point will be contained within a crown and will not receive the direct raybeam. In addition, there will be no crown centers in a cylinder of radius R around the raybeam before it reaches the point, otherwise, the point will be shaded. Since we have assumed that crown centers are distributed within boundaries h_1 and h_2 , hence the volume of this sphere and its projection toward the sun, intersected by h_1 and h_2 planes, determines the $P(n = 0 | h, \theta_i)$. We will denote this volume as V_F (Fig. 1).

Therefore, $P(n = 0 | h, \theta_i)$, the probability that no crown is centered within the volume V_F , can be obtained given the distribution of crown centers and crown geometry. For simplicity, we will assume that crown centers are randomly and independently distributed over the x, y plane and from h_1 to h_2 in height. Then $P(n = 0 | h, \theta_i) = e^{-\lambda_v V_F}$, where λ_v is the volume Poisson counts of crown centers. The calculation of $P(n = 0 | h, \theta_i)$ hence becomes the calculation of the volume V_F , which is integrated from $\Gamma(h)$ in [22]. Non-Poisson vertical distributions can also be handled at this step.

The quantity $P(n = 0 | h, \theta_i)$ can also be understood as the areal proportion of a plane at height h intercepted by sunlight that has not passed through a tree crown. Hence in a horizontal thin layer Δh , the difference $P(n = 0 | h, \theta_i) - P(n = 0 | (h - \Delta h, \theta_i))$ is the areal proportion where the solar beam first enters canopies and starts the scattering process within this thin layer Δh . We will call this the vertical distribution of directly sunlit crown surface $P(s = 0 | h, \theta_i)$, which is the areal proportion projected on the horizontal plane at the height h along solar direction.

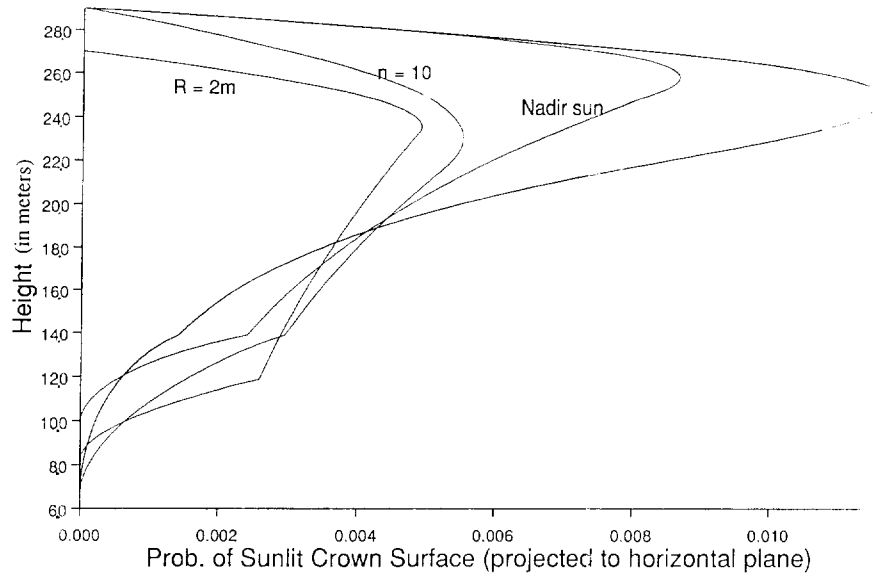


Fig. 2. Probability of sunlit crown surface. Here the default (unlabelled) curve is for a canopy composed of spherical crowns with radius $R = 4$ m that are centered randomly between heights of 10 to 25 m above the ground. Stem density is $n = 30$ per 900 m^2 providing areal coverage of 81%. The solar angle is 60 degrees. The labeled curves are for the same case, with only labeled parameter changed.

Fig. 2 shows a few examples of $P(s = 0 | h, \theta_i)$ for different illumination angles and crown geometries. Compared to homogeneous layer models, where only the top of the canopy is directly sunlit and thus its $P(s = 0 | h, \theta_i)$ should be unity at the top of the canopy and zero at any other height, we can see clearly how much the given examples depart from a homogeneous layer model. The shapes of these graphs are intuitively interpretable, given the changes in scene parameters. In the default case, only a small amount of sunlit surface occurs near the bottom of canopy. The effect of moving the sun to a nadir position reduces the amount of sunlit crown surface in the top of the canopy, but results in a slight increase toward the bottom of the canopy. Similarly, the reduction in tree crown radius or count density also has the effect of allowing more direct sunlight lower into the canopy.

V. DISTRIBUTION OF SCATTERING PATHLENGTH

Knowing the vertical distribution of sunlit crown surface, it is easy to get the pathlength distribution of sunbeams after entering a crown and traveling to a height h , i.e., $P(s' | h, \theta_i) = P(s = 0 | h + s' \cos \theta_i, \theta_i)$, where s' is the pathlength after entering the canopy. However, the real scattering pathlength (i.e., within-crown pathlength) should be smaller than s' because the sunbeam may exit the crown before reaching h .

The easiest way to get the actual scattering pathlength s from a given s' may be to calculate along the path s' the probability that a point is within a crown. But since a crown has a specific size and shape, once a sunbeam enters a crown, it will keep traveling along a segment within the crown till it exits. In other words, along the pathlength s' , the probabilities of two subsequent points are spatially correlated. Since a raybeam is attenuated exponentially along s , we need to model more accurately the scattering pathlength immediately after it enters a crown.

Knowing $P(s' | h, \theta_i)$, for any given s' , we can calculate the probability associated with the number of crowns penetrated by this pathlength, $P(n | s')$ noting that the raybeam has entered at least one crown. According to [21], the distribution $P(s | h, \theta_i)$ of scattering pathlength in discrete crown canopies can be obtained by a nested convolution process of $P(s' | h, \theta_i)$, $P(n | s')$ and $P(s | n, s')$ which is the distribution of pathlengths given the number of crowns penetrated along s' . However, at present we expect an approximation simpler than this convolution procedure would be more appropriate for understanding this mechanism. This approximation basically follows the process of convolution but replaces the innermost integral involving $P(s | n, s')$ by simple overlap mean of n crowns over s' . The procedure takes into account the fact that the scattering pathlength in the discrete canopy is determined by free overlapping of segments, and thus is accurate when s' is small, where most single scattering occurs. However, this approximation may yield some spikes when s' is large.

Fig. 3 shows $P(s | h, \theta_i)$ at different heights for a given canopy structure and illumination geometry. The peaks correspond to $n = 1, 2, 3, \dots$ respectively. The increasing pathlength of the first peak with descending height is related to the change of mean passing a single crown to reach h . The X-axis is scaled by $\cos \theta_i$ for convenience, and thus records vertical distance into the canopy.

Note that although Fig. 3 shows $P(s | h, \theta_i)$ as a set of continuous distributions, it is in fact discrete, with unequal intervals between discrete s values. Each $P(s | h, \theta_i)$ represents the average areal proportion on the h plane where the raybeam passes approximately a within-crown pathlength s .

VI. VERTICAL DISTRIBUTION OF THE SINGLE SCATTERING SOURCE

The distribution of s is obtained for all points shaded from the sun on the plane at the height h , including points both

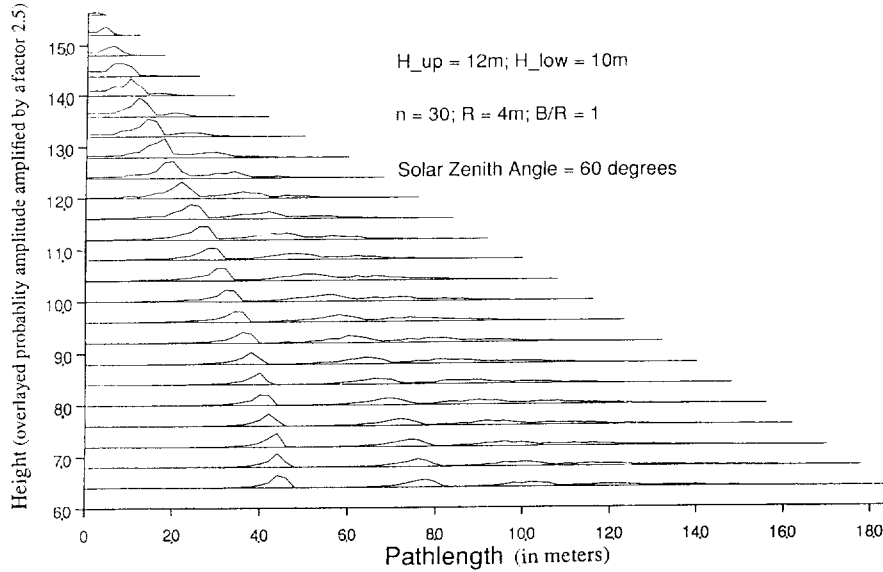


Fig. 3. Pathlength distributions at selected heights in the canopy. Each curve is probability density function (scale not shown). The X -axis for each curve is placed at the proper canopy height and the probability is shown by the curve above it with amplitude expanded by a factor of 25. All parameters are the same as the default case in Fig. 2 except that the crown centers are randomly centered between 10 m to 12 m above the ground.

inside and outside of crowns. In order to simplify the problem, here we assume the same distribution applies to both kinds of points. Then the discrete distribution of I_0 inside crowns or in shadow at height h will be the same as the distribution of s since each discrete s corresponds to a unique I_0 value, i.e., $P(I_0 | h, \theta_i) = P(s | h, \theta_i)$. Again, the intervals between consequent discrete I_0 values are unequal, determined by $\Delta s dI_0/ds$. Note that we use the physical meaning of areal proportion rather than a conventional probability density distribution because the clear relation between this areal proportion and the corresponding incoming pathlength is more important in our problem than the equality of the intervals.

$P(I_0 | h, \theta_i)$ applies to both within-crown and shaded points, but scattering happens only inside crowns. Hence the within-crown areal proportion corresponding to a certain I_0 has to be scaled by a factor: $f_B = \frac{1 - e^{-\lambda_V V_B}}{(1 - P(n=0|h, \theta_i))}$, where V_B is the volume of a sphere centered at h and intersected by h_1 and h_2 .

Knowing the areal proportion of a certain I_0 , the collided part ΔI_0 of I_0 within a thin interval Δh should have the same areal proportion as the corresponding I_0 . That is,

$$\begin{aligned} P(\Delta I_0) &= (1 - e^{-\tau \Delta s}) I_0(s | h, \theta_i) \\ &= P(I_0 | h, \theta_i) f_B. \end{aligned} \quad (5)$$

Note that this distribution is again discrete, associated with certain Δh . For reasonable values of θ_i , if we use Δh small enough, we can approximate $\Delta s = \sec \theta_i \Delta h$, as if the scattering occurs within the intersection of crowns at height h and a full depth Δh .

VII. HOTSPOT EFFECTS OF SINGLE SCATTERING

The contribution of single-scattering in canopies to the BRDF may include a strong hotspot effect that can be described at two scales: crowns and leaves.

At the scale of crowns, the hotspot comes from the correlation between $P(s | h, \theta_i)$ and $P(s | h, \theta_v)$. A special case is the correlation between $P(s = 0 | h, \theta_i)$ and $P(s = 0 | h, \theta_v)$. This correlation is the same as in our previous pure G-O model and is determined by the overlap volume $V_0(h, \theta_i, \theta_v)$ of $V_F(h, \theta_i)$ and $V_F(h, \theta_v)$. The probability that a point at h is directly sunlit and viewed will be

$$P(n = 00 | h) = e^{-\lambda_V (V_F(h, \theta_i) + V_F(h, \theta_v) - V_0(h, \theta_i, \theta_v))} \quad (6)$$

where $n = 00$ indicates no crown shades a point at height h in both directions of illumination and viewing.

Knowing $P(n = 00 | h)$, the sunlit and viewed crown surface within a thin layer Δh should have an area proportion projected along the viewing direction on the horizontal plane:

$$P_v(s = 00 | h) = \frac{P(s = 0 | h, \theta_v) P(n = 00 | h)}{P(n = 0 | h, \theta_v)}, \quad (7)$$

where $P(s = 0 | h, \theta_v)$ and $P(n = 0 | h, \theta_v)$ are analogous to $P(s = 0 | h, \theta_i)$ and $P(n = 0 | h, \theta_i)$.

Note that $P_v(s = 00 | h)$ is the areal proportion of such sunlit and viewed crown surface area in a height interval Δh , projected to a horizontal plane along the viewing direction, and its integration along h yields K_c . If the foliage area volume density goes to infinity, crown surface scattering dominates and the model will converge to our previous pure geometric-optical model for "solid crowns." $P_v(s = 00 | h)$ defines the vertical distribution of the sunlit and viewed crown surface where there is the highest positive correlation between the illumination and viewing directions. In this model we no longer assume crown surface reflection dominates. The correlation extends into the crowns, but for a given geometry, the deeper the raybeam penetrates, the weaker the correlation will be, except at the hotspot where the correlation continues to be unity along the raybeam throughout the canopy. Similarly, $P(s = 0 | h, \theta_v) - P_v(s = 00 | h)$ defines the distribution of surface area where negative correlation between scattering and

exiting attenuation dominates. The integration of this quantity along h yields K_t in our previous G-O model, defined as areal proportion of viewed crown surface in shade.

Therefore, we model the coefficient of correlation between single scattering and exiting attenuation as

$$\gamma(h) = \frac{\sum P_\nu(s=00 | z) e^{(h-z)/R}}{\sum P(s=0 | z, \theta_\nu) e^{(h-z)/R}} \quad (8)$$

where both summations are taken for all $z \geq h$. Then the total scattering contributed to a view direction ν at the height h is the sum of positively and negatively correlated means of scattering and attenuation product, weighted by the respective areal proportions.

The hotspot effect at the scale of the leaf consists of two parts. One is logically similar to the hotspot at the scale of the crown: if a raybeam reaches a point after pathlengths s without collision with a leaf, there will be no leaf centered in a volume with depth equal to s and a cross-section equal to the size of a leaf. Thus, we can model the correlation function for incidence and viewing pathlengths as a function of the overlap in this volume for the incidence path with the volume of the viewing path. This is a very sharp hotspot effect for all reasonable leaf size and FAVD. Another component of contribution from leaves to directional reflection comes from the leaf angle distribution. This contribution is modeled similar to [2, (2)], and many of other researchers' works. So we will not repeat the formulation here. Under the assumption of bilambertian reflectance and spherical leaf angle distribution, this integral has a simple analytic form [23], and will contribute a mild hotspot determined only by the phase angle between i, ν directions. However, if leaves have preferred orientation or nonbilambertian surface reflectance, this mild "hotspot" may not be at the direction backward to the sun, and digital integration may be needed. We have calculated results for such cases, but we prefer to keep the above simplified assumption unless evidence shows it to be untenable.

Then, the contribution of the single-scattering source radiance to BRDF is modeled as $I_{1+} = I_c + I_t + I_g + I_z + I_{zz}$, where I_g and I_z are contributions from directly viewed sunlit or shaded ground; I_c is the contribution from the canopy volume in the projection of K_c ; I_t is from the canopy volume in projection of K_t ; and I_{zz} is the contribution from scattering from the ground that is further attenuated by canopies before reaching the viewer. This contribution is assumed to be equally distributed over K_c and K_t , and thus should be part of the signatures C and T in our previous G-O model. The contribution of I_g may bear strong directional characteristics in sparse stands as we modeled before, and interested readers may refer to our earlier publications. Note that I_{zz} may also include a leaf-scale hotspot effect, but since usually in a forest the tree height is far larger than dimensions of leaves, such a narrow hotspot is practically undetectable, hence this effect is ignored in this model.

VIII. OPENNESS DISTRIBUTION OF DISCRETE CROWN CANOPIES

The vertical distribution of sunlit crown surface is very useful to describe the interaction of direct sunlight and crowns,

but it is directly related to a certain solar zenith angle. Frequently, we need to know in general how "open" the crown surface is to diffused skylight. Therefore we define the "openness" of a horizontal plane at the height h as the percentage of hemispherically isotropic sky irradiance passing through this plane without being intercepted by crowns. In other words

$$K_{\text{open}}(h) = \int_0^{\frac{\pi}{2}} P(n=0 | h, \theta) \sin 2\theta \, d\theta, \quad (9)$$

where θ is zenith angle taken as a variable. In a thin horizontal layer from $h - \Delta h$ to h , the proportion of hemispherical isotropic skylight entering the canopy within this layer will be

$$\Delta K_{\text{open}}(h) = \int_0^{\frac{\pi}{2}} P(s=0 | h, \theta) \sin 2\theta \, d\theta. \quad (10)$$

$\Delta K_{\text{open}}(h)$ describes how a hemispherical diffuse skylight interacts directly with crown surface at the height h . On the other hand, assuming scattering sources are randomly distributed in a thin layer at h , $\Delta K_{\text{open}}(h) / (1 - K_{\text{open}}(h))$ indicates the areal proportion of upward scattered radiation exiting the canopy without further scattering. Similarly, by ignoring the effect of trunks and assuming the symmetry of canopies to $(h_2 + h_1)/2$, $K_{\text{open}}(h_2 + h_1 - h)$ describes the direct interaction between foliage scattering and the ground surface.

At the ground, $K_{\text{open}}(h=0)$ describes how much diffused skylight reaches the ground directly without passing through tree crowns. Reciprocally, it also describes how much upward lambertian reflection from ground exits directly to the atmosphere.

This concept is important because it differentiates the behavior of the discrete crown canopy and the homogeneous layer canopy with respect to the effects of diffuse skylight and multiple scattering.

IX. MULTIPLE SCATTERING AND TOTAL DOWNWARD RADIATION TO GROUND

Knowing the distribution of single scattering source at any h , for simplicity we further assume half of the total single scattering goes upward and the other half downward at the height h in canopies

$$J_+(h) = J_-(h) = \frac{\omega}{2} \sum P(\Delta I_0 | h) \Delta I_0, \quad (11)$$

where the summation is taken for all ΔI_0 we obtained from calculating single scattering sources, and ω is the spherical albedo of leaves. On the ground, there is only upward surface scattering, so we have

$$J_+(h=0) = \rho_s [P(n=0 | h, \theta_i) I_{\text{sun}} + \sum P(I_0 | h=0, \theta_i) I_0]. \quad (12)$$

Note that here J is used to indicate radiant flux with no direction considered except upward or downward, noted by $+/-$. J has units watts/m². Part of $J_+(h)$ may directly exit

the canopy through gaps between crowns. The proportion of such upward leakage is

$$L_{k+}(h) = \frac{\Delta K_{\text{open}}(h)}{1 - K_{\text{open}}(h)} \quad (13)$$

and downward leakage will be

$$L_{k-}(h) = \frac{\Delta K_{\text{open}}(h_1 + h_2 - h)}{1 - K_{\text{open}}(h_1 + h_2 - h)}, \quad \text{for } h > h_1 - R. \quad (14)$$

At the ground, we assume $L_{k-} = 0$ and $L_{k+} = K_{\text{open}}(h = 0)$ i.e., a solid lambertian surface. This assumption can be replaced by a BRDF model of snow or soil if needed in the future. Knowing the total single scattering flux at the height h and assuming the scattering sources are spread randomly but without further leakage, the total radiation reaching another height z , $z > h$, will be

$$J_{e+}(h \rightarrow z) = (1 - L_{k+}(h))J(h) \int_0^{\pi/2} \sin(2\theta) e^{-\tau T(z, h, \theta)} d\theta, \quad (15)$$

where $T(z, h, \theta) = \sec \theta \int_h^z (1 - e^{-\lambda_v V_B(u)}) du$ is the mean pathlength from h to z along a given direction. In a thin layer centered at z , the total contribution of $J(h)$ to the next order of scattering will be

$$J_S(h \rightarrow z) = \frac{\omega}{2} (1 - L_{k+}(h))J(h) \int_0^{\pi/2} \sin(2\theta) \times (1 - e^{-\tau \Delta s}) e^{-\tau T(z, h, \theta)} d\theta, \quad (16)$$

where $\Delta s = \Delta T(z, h, \theta)$. Note the mean pathlength calculated here is different from (7)–(9), which are more accurate for small s' by taking into account the spatial correlation of pathlength segments. However, as in (22) and (23), a spike-free smooth transform from s' to s will be more appropriate. In this transform, we no longer know whether the two ends of s' are inside a crown or not, since J_s and the scattering thickness are both averaged over a thin horizontal layer including both crown cross-sections and gaps between crowns.

The contribution of $J(h)$ to the next order scattering within a thin layer centered at h itself will be

$$J_s(h \rightarrow h) = \frac{\omega}{2} (2 - L_{k+}(h) - L_{k-}(h))J(h) \times \int_0^{\pi/2} \sin(2\theta) (1 - e^{-\tau \Delta s}) d\theta, \quad (17)$$

where $\Delta s = (1 - e^{-\lambda_v V_B}) \sec \theta \Delta h / 2$.

Similarly, for any height $z < h$, we have

$$J_{e-}(h \rightarrow z) = (1 - L_{k-}(h))J(h) \times \int_0^{\pi/2} \sin(2\theta) e^{-\tau T(h, z, \theta)} d\theta \quad (18)$$

and

$$J_s(h \rightarrow z) = \frac{\omega}{2} (1 - L_{k-}(h))J(h) \int_0^{\pi/2} \sin(2\theta) \times (1 - e^{-\tau \Delta s}) e^{-\tau T(h, z, \theta)} d\theta, \quad (19)$$

When $z = 0$, i.e., at the ground surface, (25) no longer applies, since now we know that the other end of s' is on ground, which is always out of tree crowns. Therefore,

$$J_{e-}(h \rightarrow z = 0) = J(h) \int_0^{\pi/2} \sin(2\theta) \times E[P_{\text{gap}} | h_2 + h_1 - h, \theta] d\theta \quad (20)$$

where $E[P_{\text{gap}} | h_2 + h_1 - h, \theta]$ is the mean of within-crown P_{gap} , quantitatively equal to the mean attenuated irradiance I_0 , given an assumed unit of beam irradiance at direction θ as the only input. Then we have the contribution of $J(h)$ to the next order of scattering on the ground

$$J_s(h \rightarrow z = 0) = \rho_s J_{e-}(h \rightarrow z = 0) \quad (21)$$

where we also assume the ground is a smooth solid Lambertian surface and hence $J(h = 0)$ has no contribution to the next order scattering on the ground itself.

Similarly,

$$J_{e+}(h = 0 \rightarrow z) = J(h = 0) \int_0^{\pi/2} \sin(2\theta) \times E[P_{\text{gap}} | h_2 + h_1 - z, \theta] d\theta \quad (22)$$

and

$$J_s(h = 0 \rightarrow z) = \frac{\omega}{2} \Delta J_{e+}(h = 0 \rightarrow z) \quad (23)$$

The layer-source dilution function $J_s(h \rightarrow z)$ determines how the next order scattering source is distributed vertically given a scattering source at h , $J(h)$. A convolution-like operation then can be applied successively. Each time after such a dilution operation, we will obtain: 1) a vertical distribution $J^{(m+1)}(h)$ of scattering source for the next order; 2) an upward exiting radiance density $I_{m+}(\theta)$ for this order of scattering; 3) averaged total upward and downward radiation at any height within the canopy and the downward flux at the ground.

With the initial source distribution $J^{(1)}(h)$ generated by direct sunlight, we can obtain the next order scattering source distribution:

$$J^{(2)}(h) = \sum_{z=0}^{h_2+R} J_s(z \rightarrow h | J^{(1)}(h)) \quad (24)$$

where “ $|J^{(1)}(h)$ ” means given the vertical distribution of the first order scattering source. Similarly, any successive m th order of scattering can be calculated from the vertical distribution of the $(m-1)$ th order scattering source. Fig. 4 shows how the first order scattering is diluted into successive orders for different canopies. The total radiation reaching any horizontal plane h will be the superposition of these orders of radiation. Therefore the accumulated scattering source at the height h will be

$$J_{\text{acc}}(h) = \sum_{m=1}^M J^{(m)}(h), \quad (25)$$

where M is assumed large enough so that residual scattering of higher orders is small. General speaking, the more open

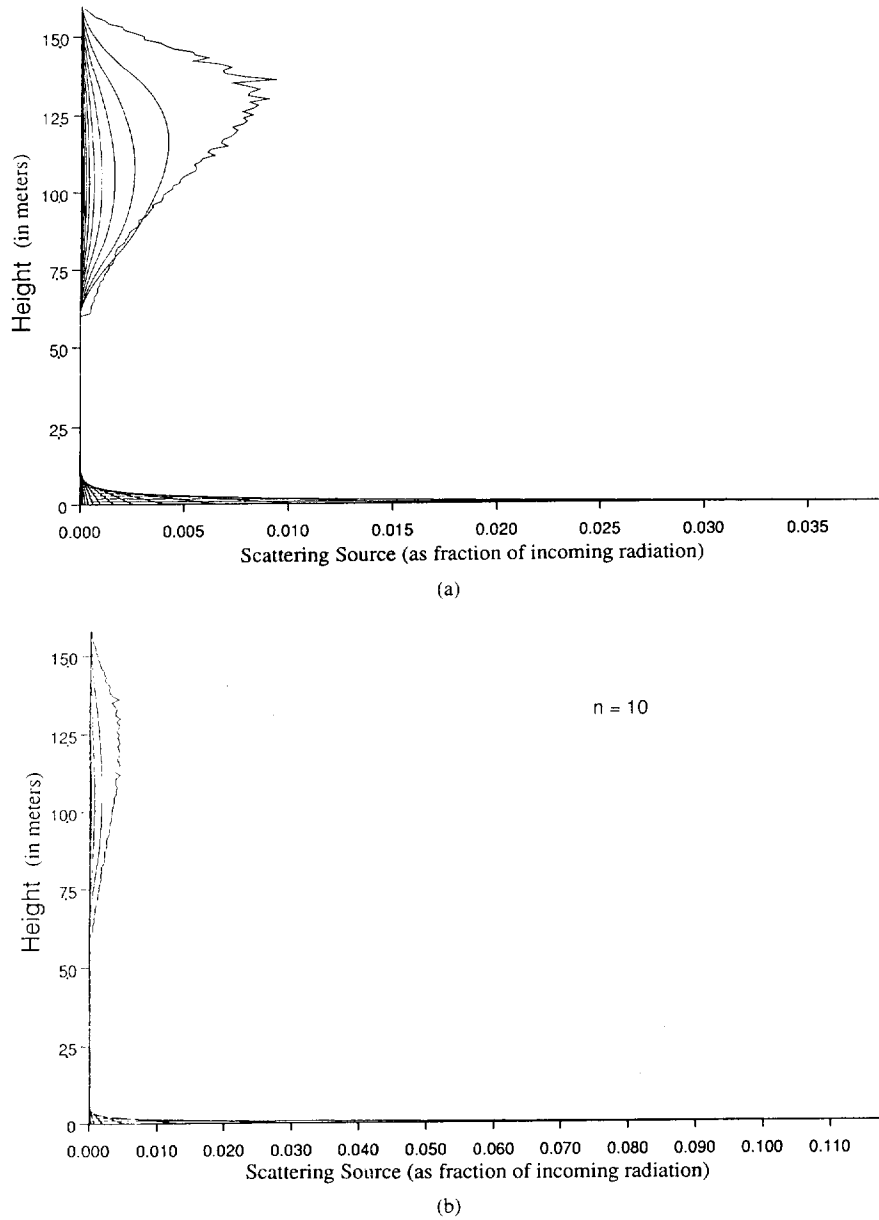


Fig. 4. Dilution of multiple scattering sources within canopy. Successive curves are for successive order of scattering with the lowest orders to the right. (a) Has the same parameters as Fig. 3, i.e., vertical coverage 81%, while projected LAI is 3, equivalent to $\tau = 0.28$ m; leaf spherical albedo $\omega = 0.972$ which makes leaf reflectance $\rho = 0.486$; ground albedo ($\rho_s =$) 0.242. (b) Changes only n to 10, resulting in a vertical coverage of 43%. The I_0 reaching the ground has been more than tripled from 15.9% to 49.3%.

the canopy, the fewer orders of scattering will be needed. For all cases we have tried, $M = 16$ has been enough, even if we set ω and ρ_s to unity (no absorption at all). However, if the canopy is totally closed and absorption is low, M would need to be larger. We may develop an estimate of needed M later, but now we assume that discrete canopies have enough openness that M does not present of a problem.

Note that accumulated source $J_{acc}(h)$ is within a thin horizontal layer Δh at any height within canopies, but it may occur at a solid surface of ground. For such acase, the total absorption will be

$$J_{abs}(h = 0) = J_{acc}(h = 0)(1 - \rho_s)/\rho_s; \quad (26)$$

and for $h > 0$

$$J_{abs}(h) = 2J_{acc}(h)(1 - \omega)/\omega. \quad (27)$$

Fig. 5 shows the total downwelling radiation to the ground surface ($J_{acc}(h = 0)$) as a function of ground albedo for several canopy structures. The effects of multiple scattering are evident in the general increase in $J_{acc}(h = 0)$ with ground albedo. Also of interest is the relative independence of $J_{acc}(h = 0)$ to the ground albedo for an open canopy with only 43% coverage. This occurs because there is little back-and-forth scattering between canopies and the ground. The lack of sensitivity of crown shapes is also interesting,

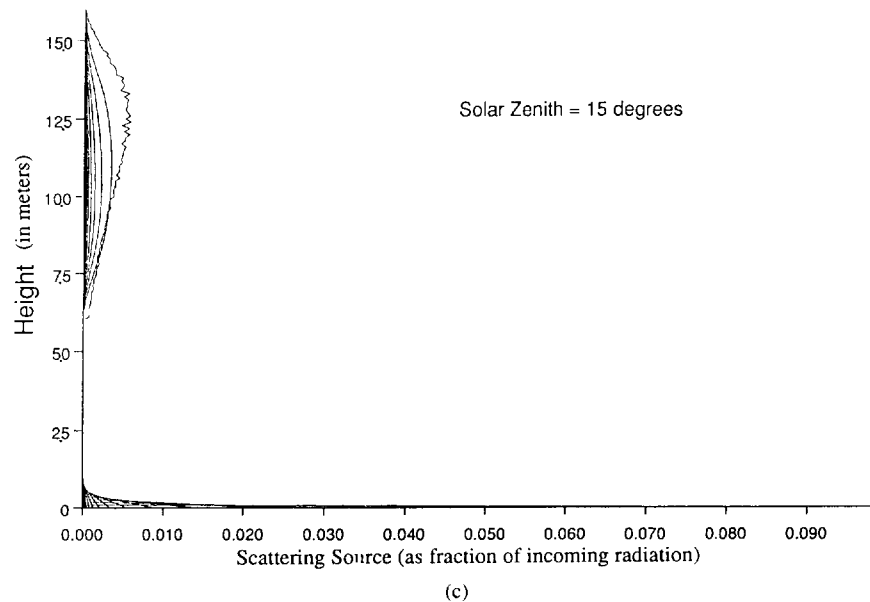


Fig. 4(cont.) (c) Changes the solar zenith angle from 60 degrees to 15 degrees, while other parameters are kept the same as (a). (c) has an uncollided solar radiation to ground about double that of (a). However, crown coverage is the same, (c) shows a similar dilution pattern as (a), while (b) has almost nothing left after the third-order scattering.

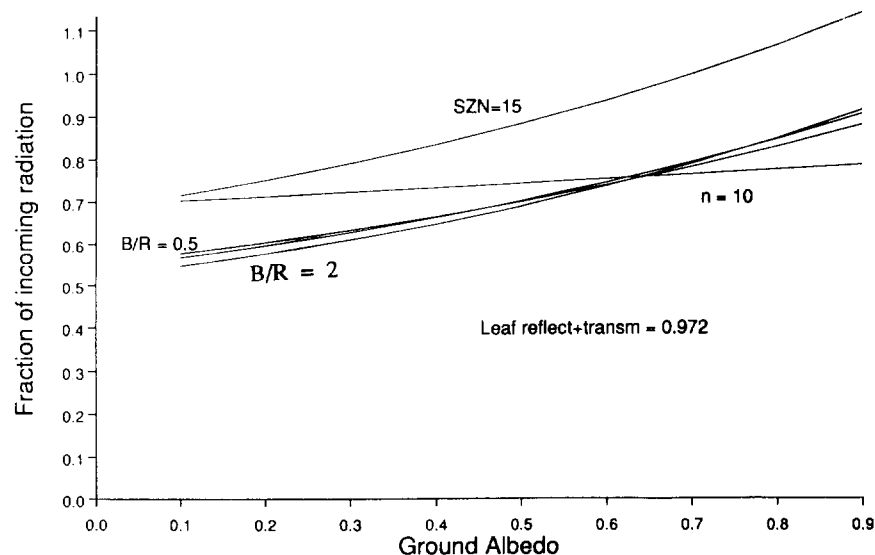


Fig. 5. Amount of radiation reaching the ground. The default parameters are the same as in Fig. 4(a). For 43% coverage ($n = 10$), the total radiation reaching the ground changes little with increasing ground albedo, because of the openness of the canopy. However, for 81% coverage, though the uncollided solar radiation is less, the total downward radiation to ground increases with ground albedo more rapidly due to the high leaf albedo (0.972) and the nearly closed canopy. At a solar zenith angle of 15 degrees, more direct uncollided sunlight penetrates to the ground, and thus the total radiation to ground is almost uniformly higher than the default curve (for solar zenith 60 degrees). Note that on this curve, the total radiation down to the ground may be greater than the total incoming radiation to this pixel, because multiple scattering is accumulated in calculating the total absorption of ground. Keeping single crown LAI unchanged (3.0) and changing crown shape via the B/R ratio, little change is noted due to a relatively sparse character of the individual crowns (low FAVD) and the relatively closed canopy.

and attributable to the high areal crown coverage and constant LAI of the examples used.

Fig. 6 shows the ground surface absorption for the same combinations of canopy structures and illumination angles. It provides both the total absorption and the portion due to multiple scattering. Again the effect of crown shapes is minimal, while the effects of the openness of the canopy and solar zenith angle are more apparent.

The above mentioned albedo or reflectance/transmittance should be understood as being spectrally dependent. The spectral albedo above the canopy will be one minus the

fraction of incoming radiation absorbed by foliage and ground. Given the incoming spectrum of illumination, the wide-band albedo above the canopy can be estimated as cited in [24].

X. VALIDATION OF THE HYBRID MODEL

In an attempt to validate the model, data from the test site in Howland, Maine were used. These data were not collected for the purpose of validating this model, and as such are less than ideal. However, these data do provide the opportunity for some investigation of the validity of the model until other data can be collected that are more appropriate. The details of the

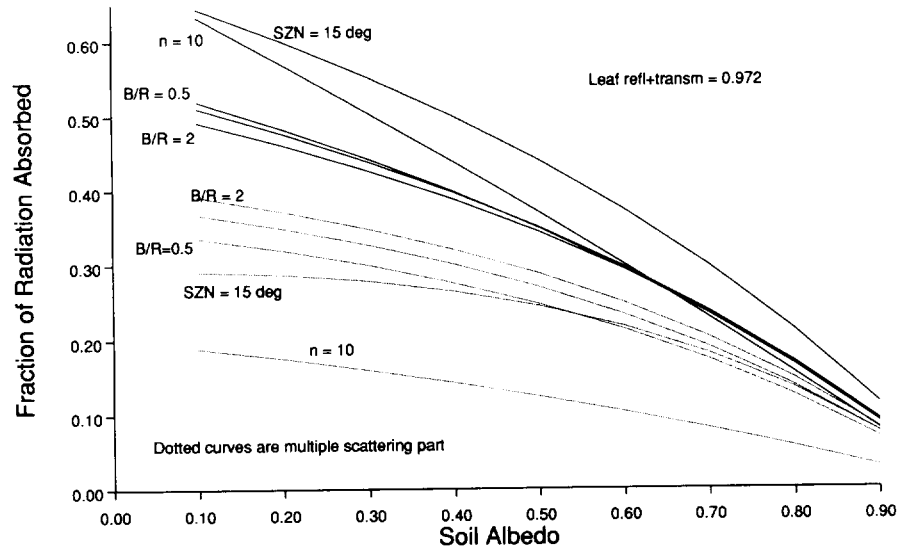


Fig. 6. Total absorption of ground surface corresponding to the five cases in Fig. 4. Dotted curves are contributions of multiple scattering, the default case remains unlabeled.

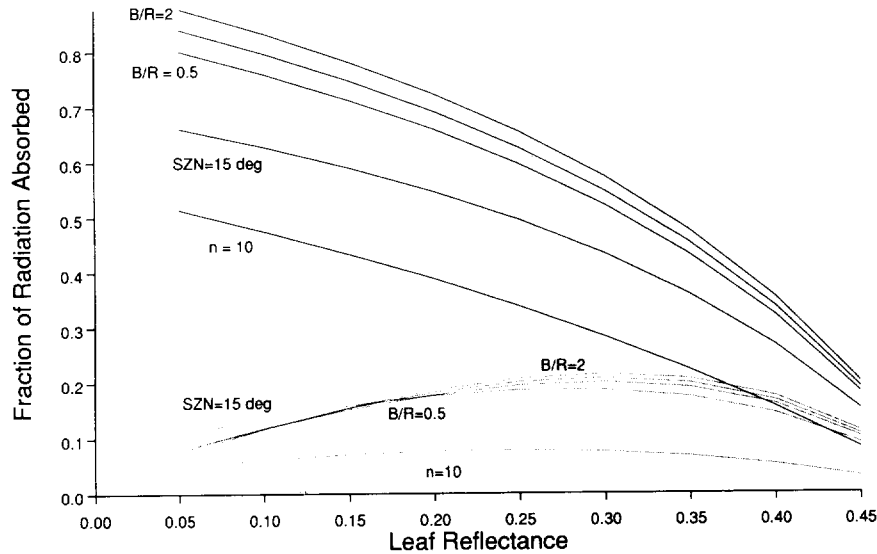


Fig. 7. Total absorption within canopies as a function of foliage reflectance (ρ) for the same cases as in Fig. 5. The default case is the unlabelled line. Note that the foliage reflectance for Figs. 4–6 is 0.486.

test site and data collection are presented in [24], [25]. The site has 1161 trees per hectare, $h_2 = 12.3$ m, $h_1 = 7.5$ m (approximated by using mean height plus/minus two standard deviations). Mean crown radius is 2.2 m and B/R ratio is 1.6. The solar zenith angle is 58.79 degrees at the time the field measurements were taken. LAI was measured using the Licor LAI-2000 instrument, 3.89 ± 0.49 according to [25].

Fig. 7 shows the total absorption of foliage for the same structures in Fig. 5, but as functions of leaf reflectance (i.e., $\omega/2$).

The spectral albedos at the solar zenith angle of 58.79 are interpolated from the PARABOLA measurements presented in [25, Fig. 12].

The field measurements of ω at the first two PARABOLA wavelengths (662 nm, 826 nm) are 0.1039, 0.9134. No field measurements are available for wavelength 1660 nm, so we have to assume a typical shape for leaf spectral reflectance and

transmittance curves, and estimate it from the values of other two wavelengths, to be approximately 0.6. The understory consists of litter, ferns, moss and grasses. The field measured ρ_s is 0.0503, 0.3248, and an estimated 0.3 at the wavelength 1660 nm. Because of the high crown coverage and large solar zenith angle, this estimate does not affect the result much.

A problem with the field data concerns the reliability of LAI measurements. The Licor instrument was designed for homogeneous canopies. When it is used for measuring LAI in forests, it encounters several problems. First, the results are not really LAI, but TPAI (Total Plant Area Index, coined in [25]). From the raw measurements, there is no way to determine the proportion of TPAI contributed by LAI. Secondly, the TPAI estimates are usually underestimated because of clustering of TPAI in tree crowns, branches and trunks. Since better measurements are not available, we made a simple assumption that LAI is one half of TPAI, but its share varies linearly

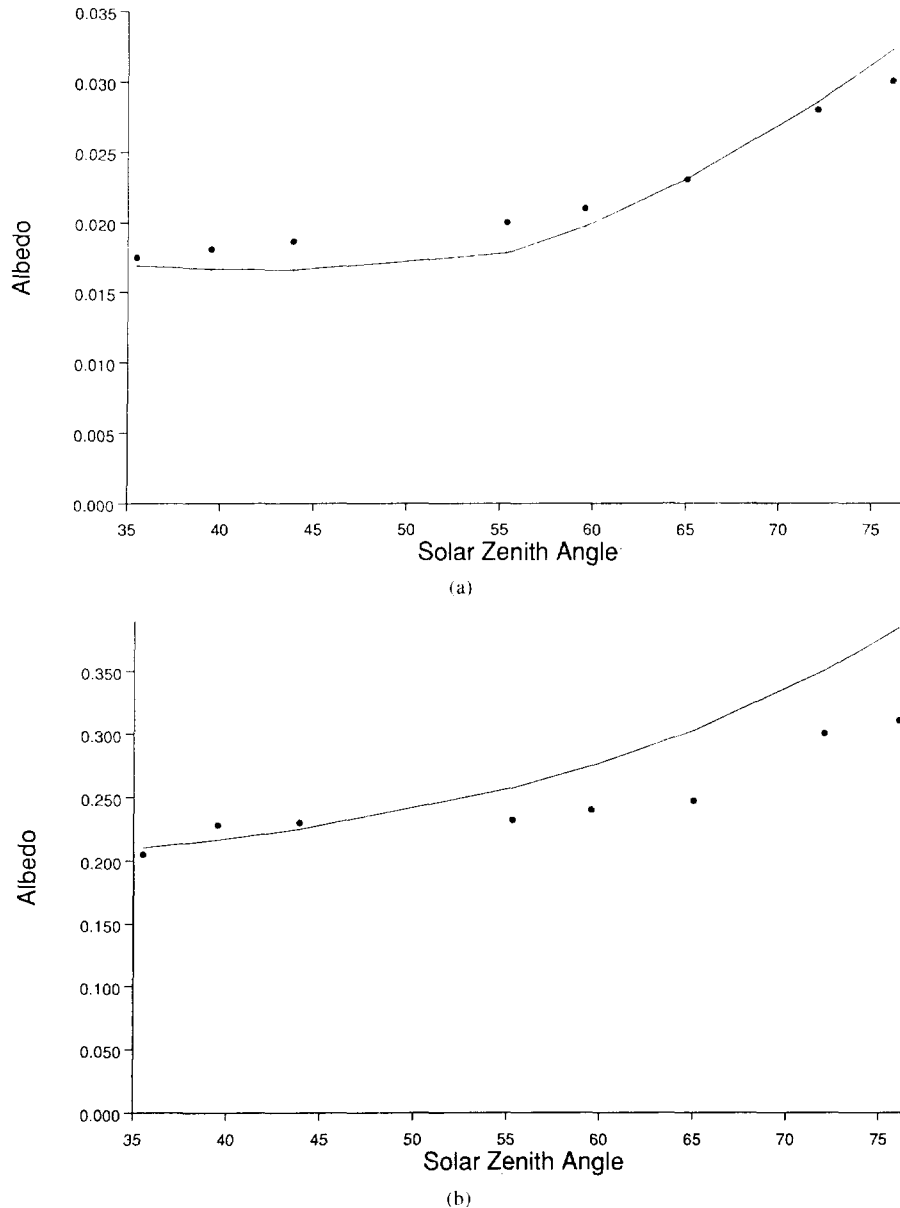


Fig. 8. Hemispherical spectral albedo. Dots are PARABOLA measurements from [25, Fig. 12]. (a) Red band (662 nm); (b) NIR (826 nm); (c) SWIR (1658 nm).

from the situation of all leaves at the top of canopy to all trunks/branches at the bottom of the canopy. Without field measurements of the spectral reflectance of trunks and branches, we further assume that they are very absorptive in all three bands. Under this assumption, we tried different TPAI values and found the results were not overly sensitive for reasonable values of TPAI. Using single crown TPAI = 6.6 (discussed further below), corresponding to $\tau = 0.70$ m, the model gives the following results: where Abs_g and Abs_f

Wavelength (nm)	Measured Albedo	Modeled Albedo	Abs_g	Abs_f
662	0.021	0.019	0.030	0.95
826	0.24	0.27	0.053	0.68
1658	0.14	0.15	0.038	0.81

are the fraction absorbed by ground and foliage respectively.

The PARABOLA measurements of albedo serve two purposes. First, they help to validate the behavior of the model on albedo estimates. The ability to estimate albedos closely at three different wavelengths using the same set of scene

parameters is encouraging. Secondly, the albedo measurements serve as a basis of comparison for estimation of TPAI. Based on the results of albedo estimation, a single crown TPAI of 6.6 was used for all future model runs and tests of directional reflectance. Fig. 8 shows the PARABOLA measurements of spectral albedo at eight different solar zenith angles, taken from [25, Fig. 12] and the model estimates.

Satisfied by the agreement between modeled albedo and PARABOLA data, we further compared the model results and PARABOLA measurements of directional reflectance, as shown in Fig. 9. For different solar zenith angles, ASAS images are used to validate the model, the fit using the same parameter set is also good [24], [26].

XI. DISCUSSION

Fig. 8 shows that the model follows the change of albedo with solar zenith angle very well in red band, reasonably well in SWIR and NIR. However, there is a general trend to overestimate albedo at large solar zenith angles in NIR

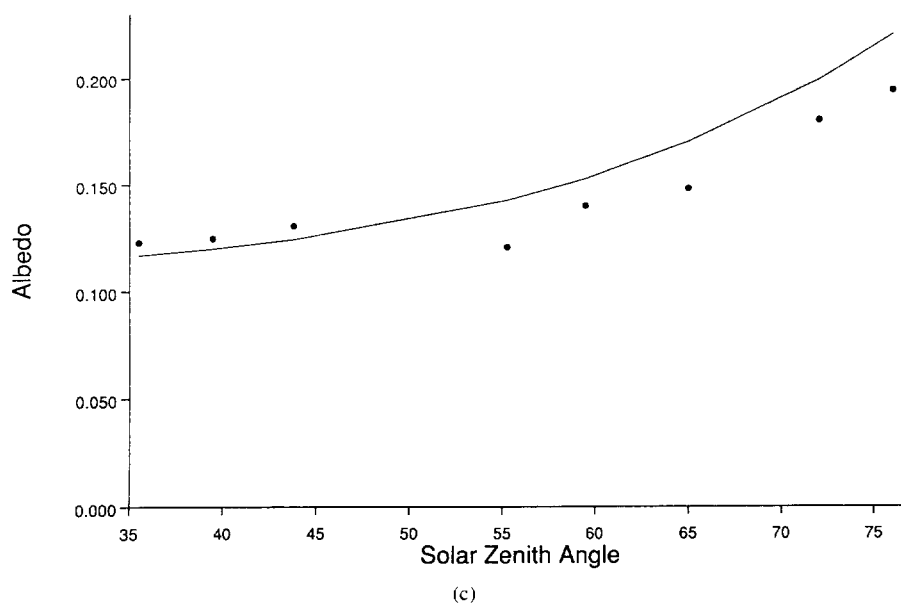


Fig. 8. (continued)

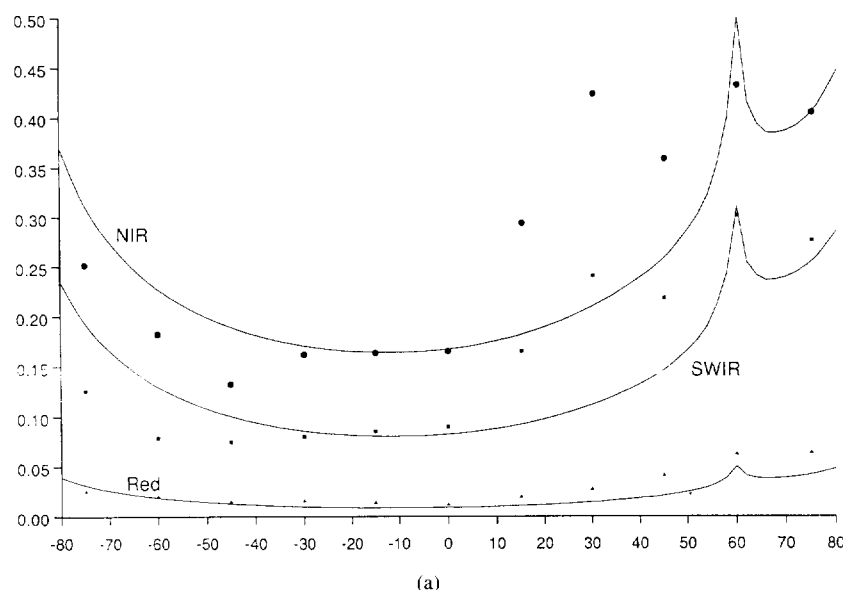


Fig. 9. Directional reflectance on the principal plane. Dots are PARABOLA measurements from [25, Table 3]. Circular dots are for NIR, square for SWIR, triangles for red. Curves are model outputs, NIR, SWIR, and red from top to bottom. (a)–(c) show three different sun angles, 59.5, 43.9, and 35.5 degrees, respectively.

and SWIR bands. This may be the result of our reasonable but simple assumption about the linear increase of share of LAI in TPAI from the bottom to the top of the crowns. This assumption in cases of NIR and SWIR bands may lead to less absorptive elements in the top of the canopy, which governs the albedo at large solar zenith angles. It also may be a result of an overestimated TPAI. The selection of the value 6.6 for TPAI proceeded from an inversion-like procedure—we changed the TPAI value and compared the model output for spectral albedos, then compared them with PARABOLA measurements at the solar zenith angle 58.79 degrees, and selected the one which fits all three bands reasonably well. However, because of the uncertainty of the share of LAI in TPAI and of the albedo of trunks and branches, no serious

attempt at inversion has been made. For example, if we assume the branches and trunks are not 100% absorptive but only absorb 95% of incident irradiation, we have much better agreement in all three bands with a TPAI value of 5.5. However, more accurate measurements for real LAI, TPAI and albedo of trunks and branches are needed before serious efforts for future analysis and inversion can be made. At present, we have to make reasonable and simple assumptions and regard TPAI as an intelligent guess instead of an inversion result.

Fig. 9 shows that the model results agree well with PARABOLA measurements in the principal plane in general trends and magnitude. But there are some disagreements, most notably in the range between nadir and the hotspot. Because

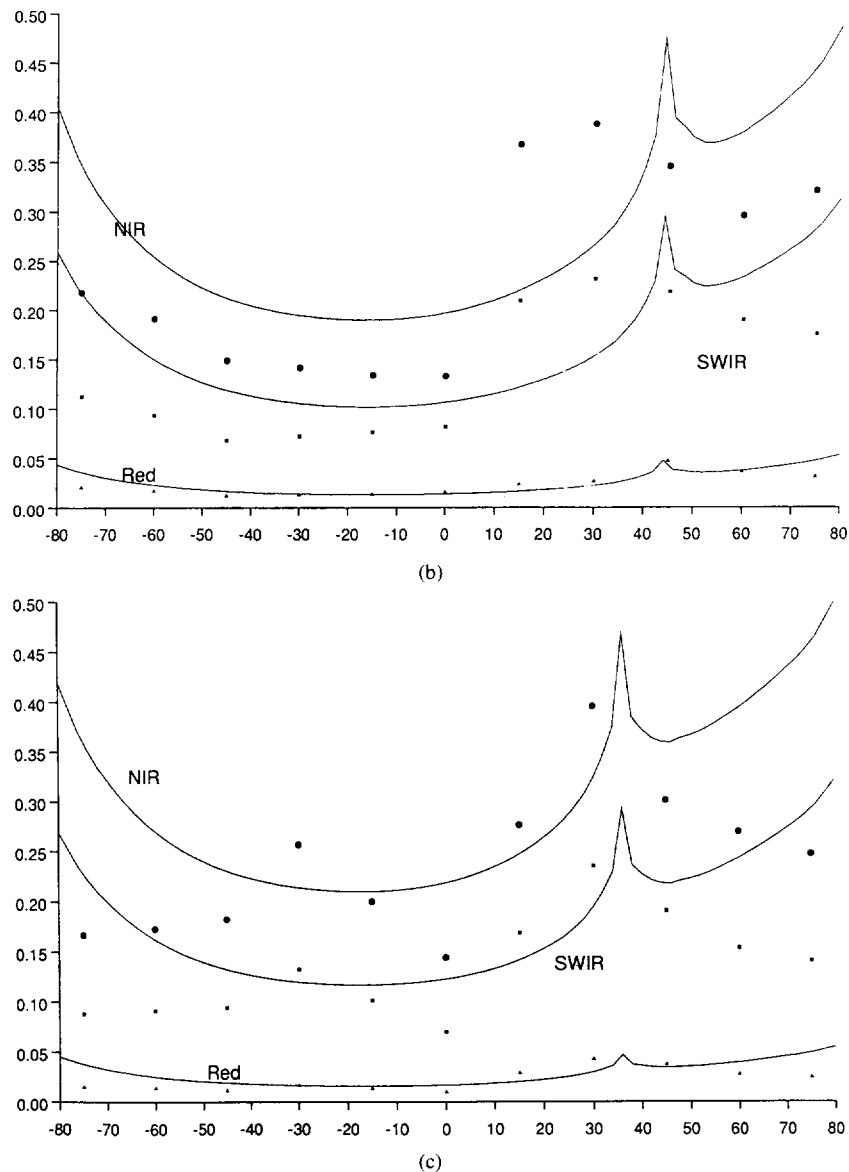


Fig. 9. (continued)

the PARABOLA measurements between the hotspot and nadir show similar patterns for all solar zenith angles, it may be that the instrument does not have a large enough FOV (field of view) to average sunlit and shaded crowns and is always looking at some sunlit crown surface at 15 and 30 degrees and is always looking at a mostly shaded spot at nadir where the FOV at the top of canopy is 2.6 m in diameter.

In order to examine this further, ASAS data were used to compare with the model results (Fig. 10). The solar zenith angle during the ASAS flight was 58.79 degrees. Only the NIR band is used (red band data were not available due to technical problems and ASAS spectral coverage does not include the SWIR band). The agreement on average value and general trend is slightly better than that of PARABOLA data. However, the model still tends to underestimate directional reflectance in the range from the hotspot to nadir and to overestimate the deep bottom of the bowl shape. In Fig. 9, the contribution of single scattering is also presented. It appears that the

directional characteristics of multiple scattering have to be considered if we need to further improve the model. One way to evaluate this concern was to compare these results with our previous attempts to model the directional reflectance of the Howland site using the pure G-O model and the field measured signatures C (0.4) and T (0.04) for sunlit and shaded crown respectively. To compare these two models, we calculated the mean contribution C_s and T_s from single scattering to the signatures C and T . We obtained $C_s = 0.22$ and $T_s = 0.02$.

It is interesting to note that the G-O model with field measured signatures provides better estimates of the directional reflectance as measured by ASAS than do the data presented in Fig. 10. It is also interesting to note that the ratios C/C_s and T/T_s ($0.4/0.22$ and $0.04/0.02$) are very close to a constant. In our present hybrid model, we treat multiple scattering as spreading over the whole horizontal plane, regardless whether it exits from sunlit or shaded crown surface or from the ground,

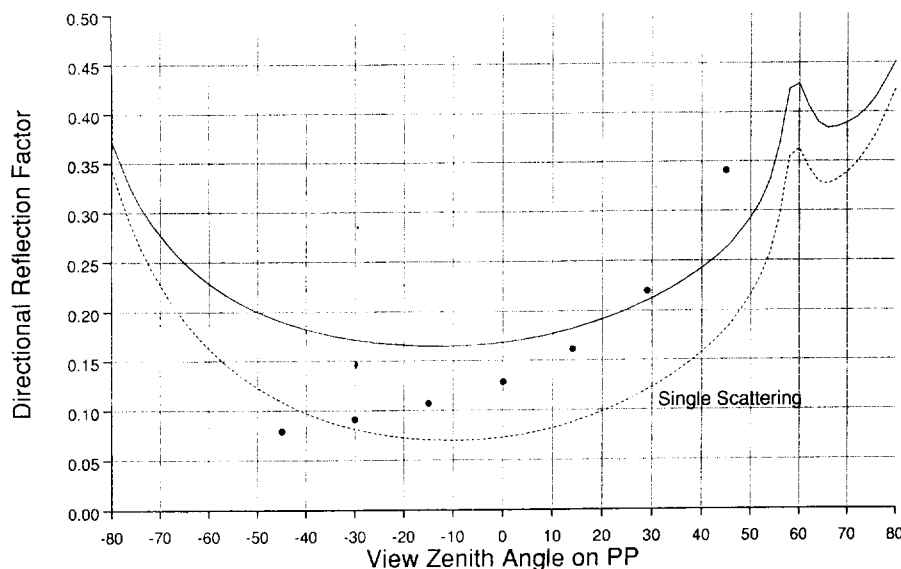


Fig. 10. Directional reflectance on the principal plane. Dots are ASAS measurements from [24]. Solid line is model output for directional reflectance; dotted line is the contribution of single scattering only.

and thus it is equivalent to model the C in the pure G-O model as $C \approx C_s + \alpha_M$ and $T \approx T_s + \alpha_M$ where α_M is the contribution of multiple scattering to the modeled albedo α . In this case α is 0.27, and α_M is 0.087. Therefore, modeled C will be smaller and modeled T will be greater than the measured values. The field measured signatures and the better fitting of G-O model both suggest that most multiple scattering still exits from the sunlit crown surface. However, we have to acquire more field measurements to conclude whether or in what cases the directional pattern of multiple scattering has to be taken into account.

We may conclude that the hybrid model works well, while further improvement can be achieved by considering the directional characteristic of multiple scattering, or from the fact that opaque and highly absorptive trunk/branch elements are not randomly distributed horizontally but concentrated in the central part of a crown, producing a much darker T than is modeled presently. However, it is unwise to make the model too complicated before more field measurements (especially LAI and TPAI distribution) are acquired and more BRDF comparisons confirm the necessity.

Fig. 9 also shows that the hybrid model gives higher reflectance at large viewing zenith angles especially for the smallest solar zenith angle (35.5 degrees) than measured values. This may be because of the simple assumption that crown centers are uniformly distributed in mean height plus/minus two standard deviations, which may overestimate mutual shading in the viewing direction. It may also result from the fact that PARABOLA is not high enough above the canopy and its FOV angle is relatively large (15 degrees), and thus it may underestimate the mutual shading effects at the large viewing zenith angles by always “seeing” some shaded crown surface. The only way these questions can be resolved is future validation and field measurements.

Diffuse sky light may play an important role in the interaction between radiation and the canopy. In fact, the concept of openness was developed from our earlier successful effort to

model the shaded ground signature Z in the case that diffuse skylight may not be ignored [27]. If the sky light is strongly specular (around the direct sun beam), we can decompose it into a set of directional irradiances with appropriate weights, and apply the theorem of superposition. In many cases, diffuse skylight (or at the least part of it) can be modeled as hemispherically isotropic, then this part can be easily added into secondary scattering source as downward scattering radiance through the $\Delta K_{\text{open}}(h)$. Since Howland data were collected under very clear sky conditions [24, Table 1], diffuse sky light is not considered in the model results in this paper in order to analyse the model’s behavior clearly.

In summary, the discrete crown canopy is characterized first by its vertical sunlit and viewed crown surface distributions and corresponding pathlength distributions. These distributions may play important roles not only in BRDF modeling, but also in many other research areas concerning forest and woodlands, such as studies of photosynthesis, soil moisture budgets, and the energy balance of snow. Then the correlation between solar direction and exiting direction is modeled at the scales of both crown and leaf. All the above are accomplished through the application of geometric optics. Then single scattering and multiple scattering are calculated according to the pathlength distributions in a way more similar to the radiative transfer approach, except that a vertical openness distribution is introduced.

Though this model may appear complicated, its final form is fairly simple and easy to apply, similar to our previous geometric-optical models. However, the component signatures needed for our previous models are now determined by the spectral scattering properties of the leaf and ground as well as the structural parameters of the plant canopies. Its simplicity may yield a promising potential in future model inversion. Though the initial validation results are encouraging, more validation efforts (especially in sparser forest canopies), and field measurements (especially distribution patterns of LAI, TPAI, crown size and tree height) are needed.

ACKNOWLEDGMENT

The authors would like to thank C. Schaaf for her work on the model inputs and Dr. D. W. Deering for generously providing a preprint of paper authored by himself, E. M. Middleton and T. F. Eck.

REFERENCES

- [1] X. Li and A. H. Strahler, "Geometric-optical modeling of a coniferous forest canopy," *IEEE Trans. Geosci. Remote Sensing*, vol. GRS-23, pp. 207–221, Sept. 1985.
- [2] ———, "Geometric-optical bidirectional reflectance modeling of mutual shadowing effects of crowns in a forest canopy," *IEEE Trans. Geosci. Remote Sensing*, vol. 30, pp. 276–292, Mar. 1992.
- [3] R. B. Myneni, J. Ross, and G. Asrar, "A review on the theory of photon transport in leaf canopies," *Agric. Forest Meteorol.*, vol. 45, pp. 1–153, 1989.
- [4] N. S. Goel, "Models of vegetation canopy reflectance and their use in estimation of biophysical parameters from reflectance data," *Remote Sens. Rev.*, vol. 4, pp. 1–222, 1988.
- [5] ———, "Inversion of canopy reflectance models for estimation of biophysical parameters from reflectance data," in G. Asrar, Ed., *Theory and Applications of Optical Remote Sensing*. New York: Wiley, 1989, pp. 205–251.
- [6] A. H. Strahler, "Vegetation canopy reflectance modeling—Recent developments and remote sensing perspectives," in *Proc. Sixth Int. Symp. Phys. Measurements Spectral Signatures*, Val d'Isere, France, January 17–21, 1994, in press.
- [7] M. M. Verstraete, B. Pinty, and R. E. Dickinson, "A physical model of the bidirectional reflectance of vegetation canopies," *J. Geophys. Res.*, vol. 95, pp. 11755–11765, 1990.
- [8] R. B. Myneni, G. Asrar, and S. A. W. Gerstl, "Radiative transfer in three-dimensional leaf canopies," *Transport Theory Stat. Phys.*, vol. 19, pp. 205–250, 1990.
- [9] D. W. Deering and P. Leone, "A sphere-scanning radiometer for rapid directional measurements of sky and ground radiance," *Remote Sens. Environ.*, vol. 19, pp. 1–24, 1986.
- [10] D. L. B. Jupp, J. Walker, and L. K. Penridge, "Interpretation of vegetation structure in Landsat MSS imagery: A case study in disturbed semi-arid eucalypt woodlands, Part 2: Model-based analysis," *J. Environ. Manag.*, vol. 23, pp. 35–57, 1986.
- [11] D. L. B. Jupp, A. H. Strahler, and C. E. Woodcock, "Autocorrelation and regularization in digital images I: Basic theory," *IEEE Trans. Geosci. Remote Sensing*, vol. GRS-26, pp. 463–473, July 1988.
- [12] ———, "Autocorrelation and regularization in digital images II. Simple image models," *IEEE Trans. Geosci. Remote Sensing*, vol. 27, pp. 247–258, May 1989.
- [13] A. H. Strahler and D. L. B. Jupp, "Modeling directional reflectance of forests and woodlands using Boolean models and geometric optics," *Remote Sens. Environ.*, vol. 34, pp. 153–166, 1990.
- [14] ———, "A hotspot model for leaf canopies," *Remote Sens. Environ.*, vol. 38, pp. 193–210, 1991.
- [15] T. Nilson, "A theory of radiation penetration into nonhomogeneous canopies, the penetration of solar radiation into plant canopies," *Acad. Sci. ESSR Rep. Tartu*, pp. 5–70, 1977.
- [16] ———, "A timber reflectance model," *Earth Res. Space*, vol. 3, pp. 63–72, 1990.
- [17] ———, "Radiation transfer in nonhomogeneous plant canopies," Abstract of Ph.D. dissertation, Tartu Univ., Tartu, Estonia, 1991.
- [18] J. R. Irons, K. J. Ranson, D. L. Williams, R. R. Irish, and F. G. Huegel, "An off-nadir pointing imaging spectroradiometer for terrestrial ecosystem studies," *IEEE Trans. Geosci. Remote Sens.*, vol. 29, pp. 66–74, 1991.
- [19] A. A. Abuelgasim and A. H. Strahler, "Modeling bidirectional radiance measurements collected by the Advanced Solid-state Array Spectroradiometer (ASAS) over Oregon transect conifer forests," *Remote Sens. Environ.*, vol. 47, pp. 261–275, 1994.
- [20] J. M. Norman and J. M. Welles, "Radiative transfer in an array of canopies," *Agron. J.*, vol. 75, pp. 481–488, 1983.
- [21] X. Li and A. H. Strahler, "Gap frequency in discontinuous canopies," *IEEE Trans. Geosci. Remote Sensing*, vol. GRS-26, pp. 161–170, Mar. 1988.
- [22] ———, "Mutual shadowing and directional reflectance of a rough surface: A geometric-optical model," in *Proc. Int. Geosci. Remote Sensing Symp.*, Clear Lake, TX, 1992, pp. 766–768.
- [23] J. Ross, *The Radiation Regime and Architecture of Plant Stands*. The Hague, Netherlands: W. Junk, 1981.
- [24] C. B. Schaaf and A. H. Strahler, "Modeling the bidirectional reflectance and spectral albedo of a conifer forest," in *Proc. 25th Int. Symp., Remote Sensing Global Environ. Change*, pp. 594–601, 1993.
- [25] D. W. Deering, E. M. Middleton, and T. F. Eck, "Reflectance anisotropy for a spruce-hemlock forest canopy," *Remote Sensing Environ.*, vol. 47, pp. 242–260, 1994.
- [26] C. B. Schaaf, X. Li, and A. H. Strahler, "Validation of bidirectional and hemispherical reflectances from a geometric-optical model using ASAS imagery and pyranometer measurements of a spruce forest," *Remote Sensing Environ.*, in press.
- [27] J. Franklin, J. Duncan, A. Huete, W. dan Leeuwen, X. Li, and A. Begue, "Radiative transfer in shrub savanna sites in Niger—Preliminary results from HAPEX-II-Sahel: I. Modeling surface reflectance using a geometric-optical approach," *Agric. Forest Meteorol.*, in press.

Xiaowen Li graduated from the Chengdu Institute of Radio Engineering, China, and received the M.A. in geography, M.S. degree in electrical and computer engineering, and the Ph.D. degree in geography from the University of California, Santa Barbara, in 1968, 1981, 1981, and 1985, respectively.

He has been Associate Professor in the Institute of Remote Sensing Application of the Chinese Academy of Science, Beijing, since 1987. He is currently Research Professor at the Center for Remote Sensing, Boston University, Boston, MA. His primary research interests are in 3-D modeling and reconstruction from multiangular remote sensed images.



Alan H. Strahler (M'86) received the B.A. and Ph.D. degrees in geography from Johns Hopkins University, Baltimore, MD, in 1964 and 1969, respectively.

He is currently Professor of Geography and Researcher in the Center for Remote Sensing, Boston University, Boston, MA. He has held prior academic positions at Hunter College of the City University of New York, New York, University of California, Santa Barbara, and at the University of Virginia, Charlottesville. He has been a Principal Investigator

on numerous NASA contracts and grants, and is currently a member of the Science Team for the EOS MODIS instrument. His primary research interests are directed toward modeling the bidirectional reflectance distribution function of discontinuous vegetation covers and retrieving physical parameters describing ground scenes through inversion of BRDF models using directional radiance measurements. He is also interested in the problem of land cover classification using multitemporal, multispectral, multidirectional, and spatial information as acquired in reflective and emissive imagery of the earth's surface.

Dr. Strahler was awarded the AAG/RSSG Medal for Outstanding Contribution to Remote Sensing in 1993.



Curtis E. Woodcock received the B.A., M.A., and Ph.D. degrees from the Department of Geography from the University of California, Santa Barbara.

Since 1984, he has taught at Boston University, Boston, MA, where he is currently Associate Professor and Chair of Geography, and a researcher in the Center for Remote Sensing. His primary current research interests in remote sensing include mapping of forest structure and change, spatial modeling of images and inversion of canopy reflectance models, detection of environmental change, and issues of map accuracy.